Journal of Microbiological Methods 85 (2011) 235–238

Contents lists available at ScienceDirect

Journal of Microbiological Methods

journal homepage: www.elsevier.com/locate/jmicmeth

Note

Synchrotron radiation infrared microspectroscopy to assess the activity of vancomycin against endocarditis vegetation bacteria

Eric Batard [a,*], Frédéric Jamme [b,c], Emmanuel Montassier [a], Dominique Bertrand [d], Jocelyne Caillon [a], Gilles Potel [a], Paul Dumas [c]

[a] Université de Nantes, EA3826 Thérapeutiques cliniques et expérimentales des infections, Nantes, France
[b] Institut National de la Recherche Agronomique, CEPIA, Nantes, France
[c] Synchrotron SOLEIL, SMIS beamline, Gif-sur-Yvette, France
[d] Institut National de la Recherche Agronomique, Equipe bioinformatique, Nantes, France

ARTICLE INFO

Article history:
Received 7 January 2011
Received in revised form 16 March 2011
Accepted 21 March 2011
Available online 5 April 2011

Keywords:
Endocarditis
Vegetation
Bacterial mass
Treatment
Vancomycin
Infrared microspectroscopy

ABSTRACT

Infrared microspectroscopy was used to show that vancomycin alters infrared spectra of endocarditis vegetation bacteria, and that vancomycin effects on bacterial biochemical contents are unevenly distributed between peripheral and central areas of bacterial masses. Infrared microspectroscopy is useful to study the activity of antibacterial agents against bacteria in tissues.

The endocarditis vegetation is mainly composed of fibrin, platelet aggregates and bacterial masses (Fowler et al., 2009). Bacterial masses grow from center to periphery, the dividing, metabolically active cells being located at their periphery. Antibiotics diffuse from the periphery of bacterial masses to their center. Hence, the center of bacterial masses is at risk to escape to antibiotic treatments for two reasons: low antibiotic concentration and reduced metabolic activity. This organization in bacterial masses could at least partly explain the poor activity of antibacterial agents in endocarditis (Moreillon and Que, 2004). However, differential effects of antibiotics against peripheral and central areas of vegetation bacterial masses have never been studied. Fourier Transform Infrared (FTIR) microspectroscopy is a powerful tool for biochemical study of tissues (Krafft et al., 2009; Miller and Dumas, 2006). Here, we used FTIR microspectroscopy to assess the effects of vancomycin on bacterial masses in an experimental endocarditis vegetation. Our objectives were (i) to determine if vancomycin alters infrared spectra of vegetation bacterial masses, and (ii) to determine if the vancomycin-induced spectral alterations are similar on central and peripheral areas of bacterial masses.

Animal experiments were carried out in accordance with European Commission Directive 86/609/EEC, and were approved by the committee of animal ethics of the University of Nantes. Endocarditis was induced as previously described (Batard et al., 2010). Three untreated rabbits were euthanized 5 days after inoculation. Two rabbits were treated by an intramuscular 40 mg/kg dose of vancomycin every 12 h at Day 4 and Day 5 after inoculation, and were euthanized 16 h after the last vancomycin injection. Vegetations were excised and cryo-sectioned in 6-μm-thick slices which were deposited on BaF2 transparent infrared windows.

A Nicolet Continuum XL microscope (Thermo Scientific, USA) was coupled to a Nicolet 5700 FTIR spectrometer using a synchrotron radiation infrared light source at SMIS beamline, Synchrotron SOLEIL, France. The microscope was equipped with a motorized sample stage and a liquid-nitrogen-cooled mercury cadmium telluride (MCT-A) detector (50 μm). It operated in a confocal mode, using a 32x infinity-corrected Schwartzschild objective (Numerical aperture = 0.65) and a matching 32× condenser. Using a double-path single-masking aperture of 8 μm × 8 μm, spectra were collected in transmission mode in the 4000 to 750 cm^{-1} mid-infrared range at a spectral resolution of 4 cm^{-1} with 128 co-added scans.

For each map, borders of the bacterial mass were determined from the visible light image. Using a Matlab home-made routine, pixels located inside these borders were classified as bacterial mass pixels, whereas pixels located outside were classified as non bacterial. For

* Corresponding author at: EA3826 Thérapeutiques cliniques et expérimentales des infections, Faculté de Médecine, 1 rue Gaston-Veil, F-44000 Nantes, France. Tel/fax: +33 240 412 854.
E-mail address: eric.batard@chu-nantes.fr (E. Batard).

0167-7012/$ – see front matter © 2011 Elsevier B.V. All rights reserved.
doi:10.1016/j.mimet.2011.03.013

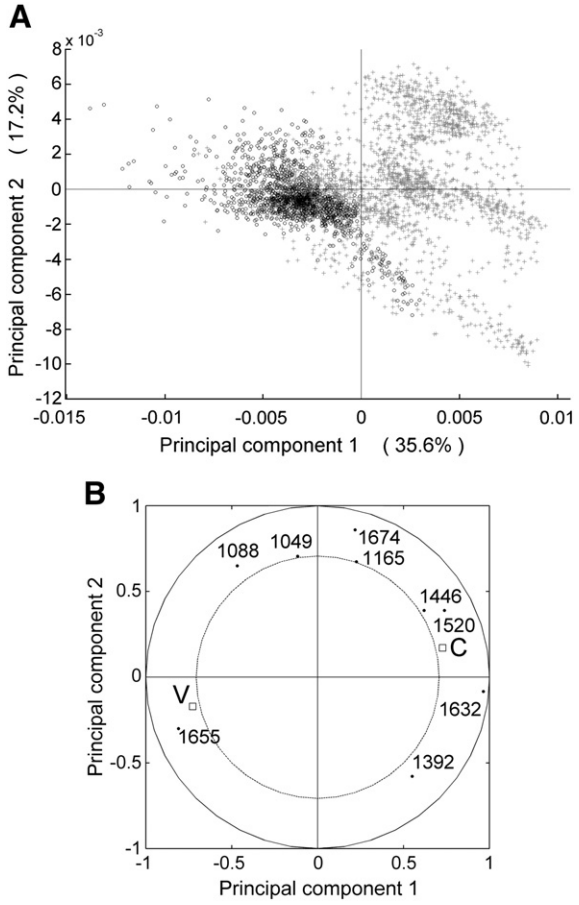

Fig. 1. Principal Component Analysis of control and vancomycin-treated vegetation bacterial masses spectra. Score plot of first and second principal components (A), shown as a function of treatment (+, control; o, vancomycin). Each point represents a spectrum. Correlation loading plot of first and second principal components (B), showing the correlation between absorbances and principal component scores. The outer and inner circles indicate respectively 100% and 50% explained variance. Only infrared bands whose variance is explained at >50% by first and second principal components are displayed. C = control; V = vancomycin. See supplementary data for colored version of Fig. 1A.

each bacterial pixel, the Euclidean distances to the border pixels were calculated, and the shortest distance was referred as the Distance from the Border of the Bacterial Mass (DBBM). Therefore, for each bacterial mass spectrum, DBBM described its spatial position within the bacterial mass. Spectra with an absorbance at 1650 cm^{-1} >1.2 were excluded in order to limit artifacts due to absorbance saturation, and spectra with an absorbance at 1650 cm^{-1} <0.4 were excluded because of unacceptable signal-to-noise ratio. After visual inspection, remaining spectra with a highly variable baseline were excluded. As a whole, less than 10% of spectra were eventually excluded from the analysis. Spectral preprocessing included consecutively smoothing using a 5 points Savitzky–Golay algorithm, second order derivation using a Savitzky–Golay 5 points algorithm with a 3rd polynomial order, and range normalization between 1780 and 980 cm^{-1}. Principal Component Analysis (PCA) and two-way ANOVA were applied to the pre-processed spectra. All map processing, data preprocessing and analysis were performed with Matlab (version R2007b) using SAISIR 2008 package of functions for chemometrics (available at http://easy-chemometrics.fr).

Thirty maps of bacterial masses were acquired (untreated rabbits, 22 maps, vancomycin-treated rabbits, 8 maps). The median (range) largest dimensions of control and vancomycin-treated bacterial masses were respectively 55 μm (27–178 μm) and 98 μm (25–150 μm) and were not statistically different (Mann–Whitney test, $P = 0.21$). 3569 bacterial mass spectra were selected (untreated, $n = 2021$; treated, $n = 1548$). DBBMs ranged from 0 to 50 μm. Preprocessed spectra were analyzed by PCA. The first and second principal components accounted respectively for 35.6% and 17.2% of the total spectral variance. Basically, control and vancomycin spectra had respectively positive and negative scores along the first principal component (PC1), and respectively positive and negative scores along the second principal component (PC2, Fig. 1A). Infrared bands whose variance is explained at >50% by PC1 and PC2 were 1674, 1655, 1632, 1520, 1446, 1392, 1165, 1088 and 1049 cm^{-1} (Fig. 1B). The projection of the treatment (control or vancomycin) on the correlation loading plot confirmed that it was highly correlated with PC1 and PC2 (Fig. 1B). For each band that correlated with PC1 and PC2 scores, bacterial mass spectra were compared by two-way ANOVA, the two factors being treatment (vancomycin or control) and DBBM (analyzed as a quantitative variable). For all wavenumbers except 1165 cm^{-1}, there was a significant interaction between treatment and DBBM, showing that the differences between control and vancomycin spectra depended on their peripheral or central location in the bacterial mass

Table 1
Relationship between spectral bands and Distance from the Border of the Bacterial Mass (DBBM). Values for second-derivative spectra. Peripheral and central areas of bacterial masses are described respectively by lower and higher values of DBBM.

			Two way ANOVA			Bonferroni post-test
Band (cm^{-1})	Status	Mean ± SE	Treatment	DBBM	Interaction	Mean difference[a] (95% CI)
1674	Control	−0.0556 ± 0.0010				
	Vancomycin	−0.0811 ± 0.0011	<0.0001	<0.0001	0.0004	−0.0255 (−0.0283, −0.0227)
1655	Control	−0.639 ± 0.0006				
	Vancomycin	−0.5817 ± 0.0007	<0.0001	0.0056	0.0021	0.0573 (0.0554, 0.0591)
1632	Control	−0.0575 ± 0.0015				
	Vancomycin	−0.1866 ± 0.0017	<0.0001	0.0002	<0.0001	−0.1291 (−0.1334, −0.1247)
1520	Control	−0.1359 ± 0.0005				
	Vancomycin	−0.1734 ± 0.0005	<0.0001	<0.0001	0.0001	−0.0375 (−0.0389, −0.036)
1446	Control	−0.0753 ± 0.0002				
	Vancomycin	−0.0861 ± 0.0003	<0.0001	<0.0001	<0.0001	−0.0107 (−0.0114, −0.0101)
1392	Control	−0.1001 ± 0.0003				
	Vancomycin	−0.1091 ± 0.0004	<0.0001	<0.0001	<0.0001	−0.009 (−0.0099, −0.008)
1165	Control	−0.0271 ± 0.0003				
	Vancomycin	−0.0378 ± 0.0004	<0.0001	<0.0001	0.5506	−0.0107 (−0.0117, −0.0097)
1088	Control	−0.0867 ± 0.0007				
	Vancomycin	−0.0624 ± 0.0008	<0.0001	<0.0001	<0.0001	0.0243 (0.0221, 0.0265)
1049	Control	−0.0314 ± 0.0006				
	Vancomycin	−0.0341 ± 0.0007	0.5068	<0.0001	0.0001	−0.0027 (−0.0045, −0.001)

[a] Difference between vancomycin and control spectra.

(Table 1). Post-test comparisons showed that vancomycin and control spectra were significantly different for all tested bands (Table 1). The interaction between treatment and DBBM is detailed in Fig. 2. The effect of vancomycin was more intense at the periphery of the bacterial masses (i.e. for lower DBBMs) than in their center (i.e. for higher DBBMs) for bands at 1632, 1520, 1446, 1392 and 1088 cm^{-1}. Conversely, the effect of vancomycin was more intense at the center of the bacterial masses than in their periphery for bands at 1674, 1655 and 1049 cm^{-1}.

Additionally, 523 non bacterial mass spectra were selected (untreated, $n=335$; treated, $n=188$) and analyzed by PCA. The first and second principal components accounted respectively for 58.6% and 11.1% of the total spectral variance. However, they did not discriminate control and vancomycin spectra (data not shown).

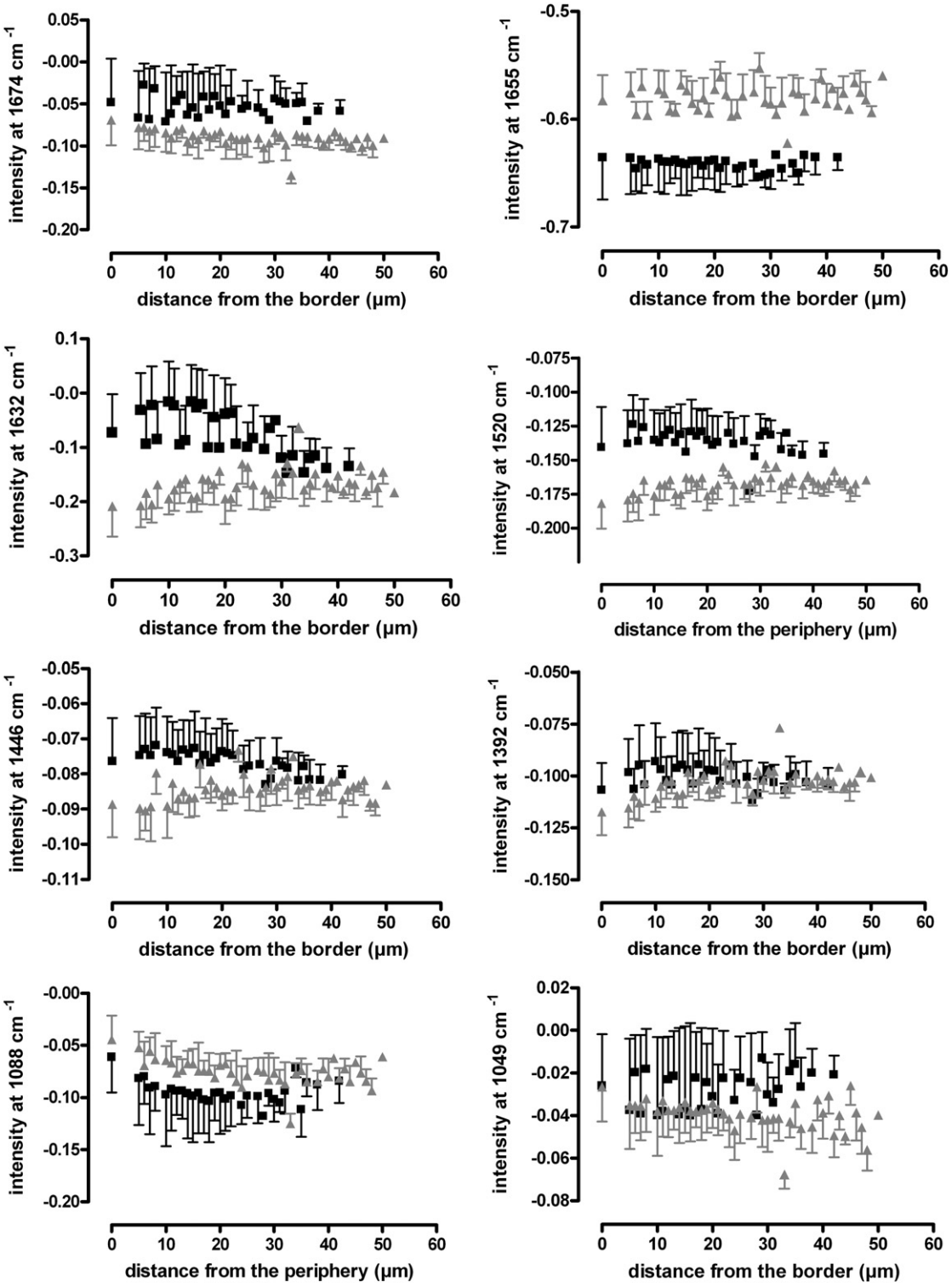

Fig. 2. Relationship between preprocessed spectral bands and distance from the border of the bacterial mass (DBBM).Peripheral and central areas of bacterial masses are described respectively by lower and higher values of DBBM.Black = control, gray = vancomycin. Mean values are shown; bars represent SD.

Our study demonstrates that vancomycin alters infrared spectra of vegetation bacterial masses. PCA discriminated control and vancomycin bacterial mass spectra, whilst it did not for non bacterial spectra. Furthermore, vancomycin major infrared bands were not increased in vancomycin-treated tissues (data not shown). Then, alterations of bacterial spectra plausibly result from vancomycin-induced modifications of the biochemical content of bacterial masses. The 1088 cm^{-1} band is an infrared marker for phosphates, that are mainly present in bacterial nucleic acids and teichoic acids (Jiang et al., 2004). The 1165 and 1049 cm^{-1} bands are related to carbohydrates and to peptidoglycan (Naumann et al., 1982). Bands at 1674, 1655 and 1632 cm^{-1} are related to protein secondary structure, and bands at 1446 cm^{-1} and 1392 cm^{-1} are attributed to CH3 groups in fatty acids (Batard, et al., 2010; Kong and Yu, 2007). There was a spatial gradient between bacterial mass peripheral and central areas for most of vancomycin-induced spectral alterations. Vancomycin increased protein beta-turn (1674 cm^{-1}) and carbohydrate contents (1049 cm^{-1}) mainly in the bacterial mass center, thus showing that vancomycin diffuses to the bacterial masses center. Conversely, vancomycin-induced spectral alterations related to protein beta-sheet (1632 cm^{-1}), fatty acids (1446 and 1392 cm^{-1}), and phosphates (1088 cm^{-1}) were mainly observed in bacterial masses periphery.

FTIR spectroscopy has previously been used to assess the biochemical effects of various antibacterial agents against bacteria grown in broth (Al-Qadiri et al., 2008; Bizani et al., 2005; Motta et al., 2008; Zeroual et al., 1995). For the first time, we show that FTIR microspectroscopy can be used to assess the biochemical effects of antibiotics against bacteria in an infected tissue. The synchrotron source provided a highly brilliant infrared radiation which allowed to lower the microscope aperture to 8 μm × 8 μm with a good signal-to-noise ratio even at low wavenumbers. Thanks to this optimal spatial resolution, we could explore the biochemical structure of bacterial masses. By showing different biochemical effects on peripheral and central areas of streptococcal masses, this study supports the hypothesis that vancomycin activity on bacterial viability may depend on the location within the bacterial mass.

Supplementary materials related to this article can be found online at doi:10.1016/j.mimet.2011.03.013.

Acknowledgment

This work was partially funded by the Synchrotron Soleil (proposal 20080735). The funding source had no role in study design, collection, analysis and interpretation of data, in the writing of the report, and in the decision of submit the paper for publication.

References

Al-Qadiri, H.M., Al-Alami, N.I., Al-Holy, M.A., Rasco, B.A., 2008. Using Fourier transform infrared (FT-IR) absorbance spectroscopy and multivariate analysis to study the effect of chlorine-induced bacterial injury in water. J. Agric. Food Chem. 56, 8992–8997.

Batard, E., Jamme, F., Boutoille, D., Jacqueline, C., Caillon, J., Potel, G., Dumas, P., 2010. Fourier Transform Infrared Microspectroscopy of endocarditis vegetation. Appl. Spectrosc. 64, 901–906.

Bizani, D., Motta, A.S., Morrissy, J.A., Terra, R.M., Souto, A.A., Brandelli, A., 2005. Antibacterial activity of cerein 8A, a bacteriocin-like peptide produced by *Bacillus cereus*. Int. Microbiol. 8, 125–131.

Fowler Jr., V.G., Scheld, W.M., Bayer, A.S., 2009. Endocarditis and intravascular infections. In: Mandell, G.L., Bennett, J.E., Dolin, R. (Eds.), Principles and practice of infectious diseases, Vol. 1. Churchill Livingstone Elsevier, Philadelphia, pp. 1067–1112.

Jiang, W., Saxena, A., Song, B., Ward, B.B., Beveridge, T.J., Myneni, S.C., 2004. Elucidation of functional groups on gram-positive and gram-negative bacterial surfaces using infrared spectroscopy. Langmuir 20, 11433–11442.

Kong, J., Yu, S., 2007. Fourier transform infrared spectroscopic analysis of protein secondary structures. Acta Biochim. Biophys. Sin. (Shanghai) 39, 549–559.

Krafft, C., Steiner, G., Beleites, C., Salzer, R., 2009. Disease recognition by infrared and Raman spectroscopy. J. Biophotonics 2, 13–28.

Miller, L.M., Dumas, P., 2006. Chemical imaging of biological tissue with synchrotron infrared light. Biochim. Biophys. Acta 1758, 846–857.

Moreillon, P., Que, Y.A., 2004. Infective endocarditis. Lancet 363, 139–149.

Motta, A.S., Flores, F.S., Souto, A.A., Brandelli, A., 2008. Antibacterial activity of a bacteriocin-like substance produced by *Bacillus* sp. P34 that targets the bacterial cell envelope. Antonie Van Leeuwenhoek 93, 275–284.

Naumann, D., Barnickel, G., Bradaczek, H., Labischinski, H., Giesbrecht, P., 1982. Infrared spectroscopy, a tool for probing bacterial peptidoglycan. Potentialities of infrared spectroscopy for cell wall analytical studies and rejection of models based on crystalline chitin. Eur. J. Biochem. 125, 505–515.

Zeroual, W., Manfait, M., Choisy, C., 1995. FT-IR spectroscopy study of perturbations induced by antibiotic on bacteria (*Escherichia coli*). Pathol. Biol. (Paris) 43, 300–305.